Highly efficient green polymer light-emitting diodes through interface engineering

Qianfei Xu
Jinsong Huang
Yang Yang

Abstract — By interface engineering, we have improved the quantum efficiency for green polyfluorene polymer light-emitting diodes by three fold: the efficiency improved from 9 to 28 cd/A. This interface engineering was achieved by inserting a thin layer of calcium (2) acetylacetonate, denoted as $Ca(acac)_2$, at the polymer/metal cathode interface. The $Ca(acac)_2$ layer behaves in a multifunctional way. It assists the electron injection by lowering the electron-injection barrier. In the meanwhile, hole injection is enhanced by the accumulated electrons in the polymer layer. This effect is believed to lower the barrier height for hole-injection through the Schottky effect. Finally, the $Ca(acac)_2$ layer works as a hole block layer to block the holes. As a result of the charge balance and charge confinement, the device quantum efficiency increases dramatically.

Keywords — *Organic electronics, interface engineering, PLEDs, $Ca(acac)_2$, green polyfluorene.*

1 Introduction

Since the discovery of polymer light-emitting diodes (PLEDs),[1] considerable attention has been attracted by their increasing potential for applications as displays and solid-state lighting sources. Polymer electroluminescence (EL) is an interesting phenomenon involving several physical steps, including injection, transport, and recombination of positive and negative charges inside a luminescent polymer thin film with the bandgap in the visible range. The optimization of device performance (efficiency) requires an improvement in the luminescence efficiency of the emitting material, and a well-balanced injection of positive and negative charge carriers.[2] Therefore, optimization of the interface plays an important role in improving the device performance. An unbalanced charge injection often happens due to the different barrier heights at the anode and cathode interfaces. This causes an excess of one carrier, which leads to low recombination yield and consequently low quantum efficiency. The interface engineering thus becomes very important in order to improve the device efficiency.

In general, a thin layer of conducting polymer is used to modify the anode interface,[3,4] while low-work-function metals, such as calcium, are often used to reduce the barrier height at the cathode interface.[5,6] However, low-work-function metals are susceptible to degradation due to their high chemical reactivity with oxygen and moisture. It is therefore crucial to find a reliable material to modify the interface to get good electron injection. In addition to charge balance, another important effect in the polymer EL process is the space-charge effect, which is often caused by the low carrier mobility in the polymer layer. For example, significant amount of literature have reported that operation of poly(p-phenylenevinylene) (PPV) based LEDs depends on not only the injection barriers but also the space-charge effects.[7–9] For polyfluorenes,[10–13] the space-charge effect has also been reported playing an important role for affecting the device performance.[14]

In this manuscript, we present a simple model, based on our characterizations, to explain the significant efficiency improvement of the green polyfluorene PLEDs *via* interface engineering at the cathode contact. The characterizations include the *I–V* curve studies of the devices with different architectures, photovoltaic measurements, and the impedance characterization.

2 Experiment

Our PLEDs were fabricated on pre-cleaned glass substrates coated with high-work-function indium tin oxide (ITO) as the anode. A buffer layer of 50 nm poly(ethylene dioxy thiophene)/polystyrene sulfonate (PEDOT:PSS) was used as a hole-injection layer at the anode interface, between ITO and the emission polymer. The emitting polymer layer was fabricated by spin-coating, inside a pure nitrogen-filled glove box. The polymer we used is a blended polymer (5BTF8), consisting of 5-wt.% poly (9,9-dioctylfluorene-co-benzothiadiazole) (denoted by BT) and 95-wt.% poly (9,9-dioctylfluorene) [denoted by PFO, see Fig. 1(a) for the chemical structure]. Aluminum (Al) was deposited by thermal evaporation under 10^{-6}-torr vacuum as the electron-injecting contact (cathode). The efficiency enhancement of our device was achieved by inserting a nanoscale interfacial modification layer made of calcium (2) acetylacetonate [$Ca(CH_3COCHCOCH_3)_2$], denoted as [$Ca(acac)_2$], between the polymer and Al.[15,16] The chemical structure of $Ca(acac)_2$ is shown in Fig. 1(b). The $Ca(acac)_2$ is a 0.2 wt.% (0.2 mg/ml) solution in ethoxyethanol solvent, with polyoxyetholene(12) tridecyl ether ($C_{13}H_{27}(OCH_2CH_2)_n$ OH) as surfactant to enhance adhesion to the 5BTF8 polymer. In order to clarify the role of this interfacial layer,

Received 01/08/05; accepted 01/25/05

The authors are with the Department of Materials Science and Engineering, University of California, Los Angeles, CA 90095, U.S.A.; telephone 310/825-4052, e-mail: yangy@ucla.edu.

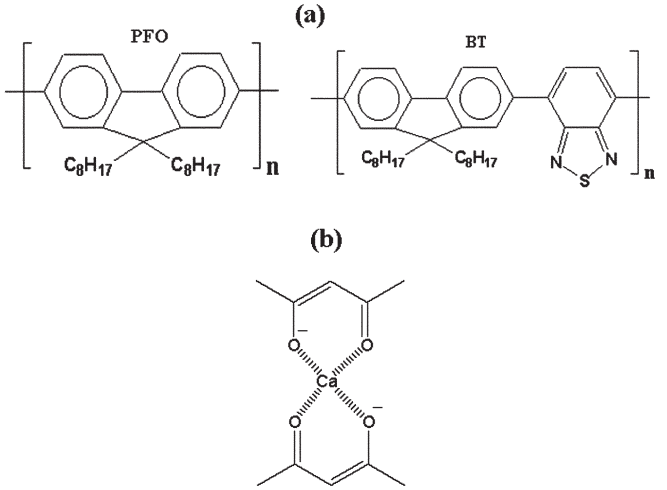

FIGURE 1 — (a) Chemical structure of the green polymer, which is a blended polymer (5BTF8), consisting of 5-wt.% poly (9,9-dioctylfluorene-co-benzothiadiazole) and 95-wt.% poly (9,9-dioctylfluorene). (b) The chemical structure of $Ca(acac)_2$.

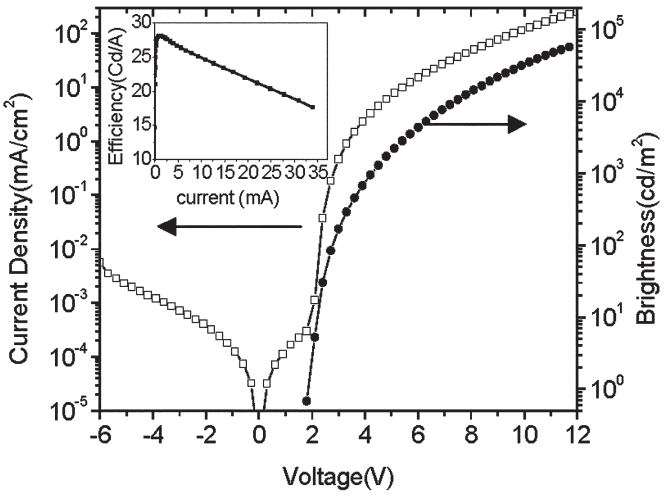

FIGURE 2 — The *I–V–L* curve of the device with $Ca(acac)_2$ as the interfacial modification layer. The inset is the plot of luminance efficiency *vs.* current.

$Al(acac)_3$, $Ba(acac)_2$, and $Mg(acac)_2$ were used to substitute the $Ca(acac)_2$ layer, while Au and Cu were used to substitute the Al electrode, respectively. Conventional devices using Ca/Al as cathode were made as reference devices. In the interim, the electron-only devices were fabricated by replacing high-work-function ITO with low-work-function Ca at the anode to study the electron injection. All the PLEDs reported in this manuscript were fabricated from solutions in *p*-Xylene, with a concentration of 10 mg/ml. All the solutions mentioned above were prepared in a glove box with N_2 ambient. The PLED characterization was carried out by a Keithley 2400 source- measure unit and a calibrated silicon photodiode. The brightness was further measured by using a Photo Research PR650 spectrophotometer. Impedance and capacitance– voltage (*C–V*) measurements were carried out with a frequency-response analyzer, HP 4284A Precision LCR meter. The complex ac impedance, Z, was recorded at test frequencies between 20 and 10^6 Hz at a range of different applied biases. An ac signal with a 30-mV amplitude was superimposed with dc bias. All devices were tested in nitrogen ambient.

3 Results and discussion

The improvement in device efficiency is believed to have resulted due to several effects, such as the enhancement in electron-injection due to the $Ca(acac)_2$ layer, the enhancement in hole injection due to the accumulated electron density (electron-induced hole injection), and finally, hole blocking (or confinement) due to the $Ca(acac)_2$ layer. In the following sessions, we will present the experimental results and modeling.

3.1 Increased efficiency by the application of $Ca(acac)_2$ interfacial layer

Figure 2 shows the *I–L–V* (current–brightness–voltage) curves of PLEDs with the $Ca(acac)_2$ interfacial layer, the inset is a plot of the luminance efficiency *vs.* current. The device turn-on voltage is around 1.8 V. The luminance efficiency reaches 28 cd/A, the corresponding current density is around 10 mA/cm^2, while the corresponding luminance is around 2650 cd/m^2. By comparing the *I–L–V* curves of $Ca(acac)_2$-based devices and conventional Ca-based devices, it was found that device current turn-on voltages were almost the same while the light turn-on voltages of the $Ca(acac)_2$-based device was lower than that of the Ca-based device (see Ref. 16 for details). We also fabricated the device using gold as the over-coating metal layer and found that the device performance was similar to that with Al as the over-coating metal. Hence, the $Ca(acac)_2$ interfacial layer is obviously a key factor for the significant improvement of the device performance. In addition, we have also tried $Al(acac)_3$, $Mg(acac)_2$, and $Ba(acac)_2$ and these compounds show similar device performance as the $Ca(acac)_2$ device.

In the polymer diodes with low conductivity materials, such as polyfluorene, the open-circuit voltage (V_{oc}) is determined by the difference of the work functions of the two electrodes. Hence, photovoltaic measurements have been performed to investigate the open circuit voltages of devices with different compounds as the interfacial layer. The results are shown in Fig. 3. It is clearly shown that the work function of the cathode contacts of $Mg(acac)_2$, $Ca(acac)_2$, and $Ba(acac)_2$ are close to the corresponding metals. These results are consistent with the *I–V–L* results from PLED, which indicates that the $Ca(acac)_2$/Al interface provides a similar work function as that of the pure Ca electrode.

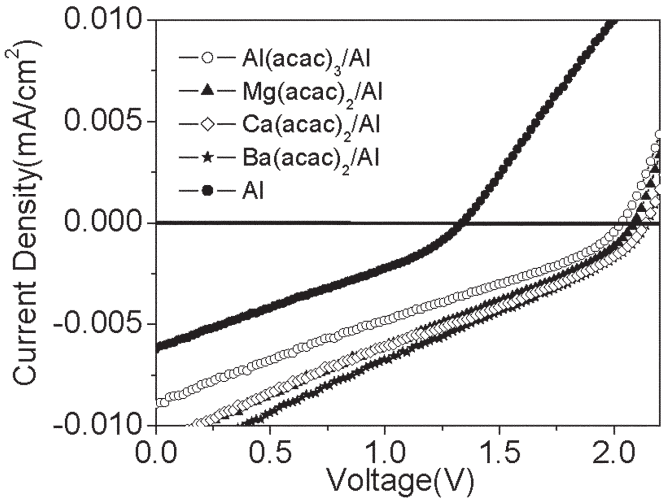

FIGURE 3 — The photovoltaic results of Al, Al(acac)$_3$, Mg(acac)$_2$, Ca(acac)$_2$, and Ba(acac)$_2$. All of the metal(acac)$_x$ compounds were overcoated with Al.

3.2 Improved electron injection by Ca(acac)$_2$ interfacial layer

In order to understand the device mechanism for the improved efficiency, we first study the effect of Ca(acac)$_2$ interface on the electron injection. An ideal approach to analyze the electron injection of the device is to study the *I–V* curves of the electron-only devices.[17] In the electron-only device, the ITO anode contact is replaced by a low-work-function metal such as Ca, while the cathode contact is kept the same as normal devices. Due to the large offset between the Fermi level of Ca (around 2.9 eV) and HOMO (highest-occupied molecule orbital) of the polymer (about 5.8 eV), the injection of holes can be neglected in the device. As a result, the current in the device can be considered to be caused only by electron injection.

In our experiments, we made the electron-only devices based on both Ca(acac)$_2$/Al contact and Ca/Al contact. The comparison of the *I–V* curves is shown in Fig. 4(a). At the same voltage (or electrical field), a dramatic current-density increase is observed in the Ca(acac)$_2$-based device, compared to that in the Ca-based device. This indicates that the Ca(acac)$_2$ layer facilitates the electron injection more efficiently compared to the Ca cathode. In our previous work,[16] we have attributed the effect of Ca(acac)$_2$ as a chemical reaction which enables the Ca(acac)$_2$/Al electrode to have a similar work function as the Ca/Al electrode. (The chemical reaction is supported by the XPS results, which are not shown here.) However, judging by the data from the electron-only devices, it seems like we cannot fully explain the higher electron injection of Ca(acac)$_2$ electrode by chemical reaction itself. (Otherwise, the data should be similar or identical. The difference of current at lower voltages is more than one order of magnitude; hence, it is beyond experimental error.) Therefore, in addition to the chemical reaction, one must consider another physical mechanism, the assist-tunneling caused by the thin Ca(acac)$_2$ layer.

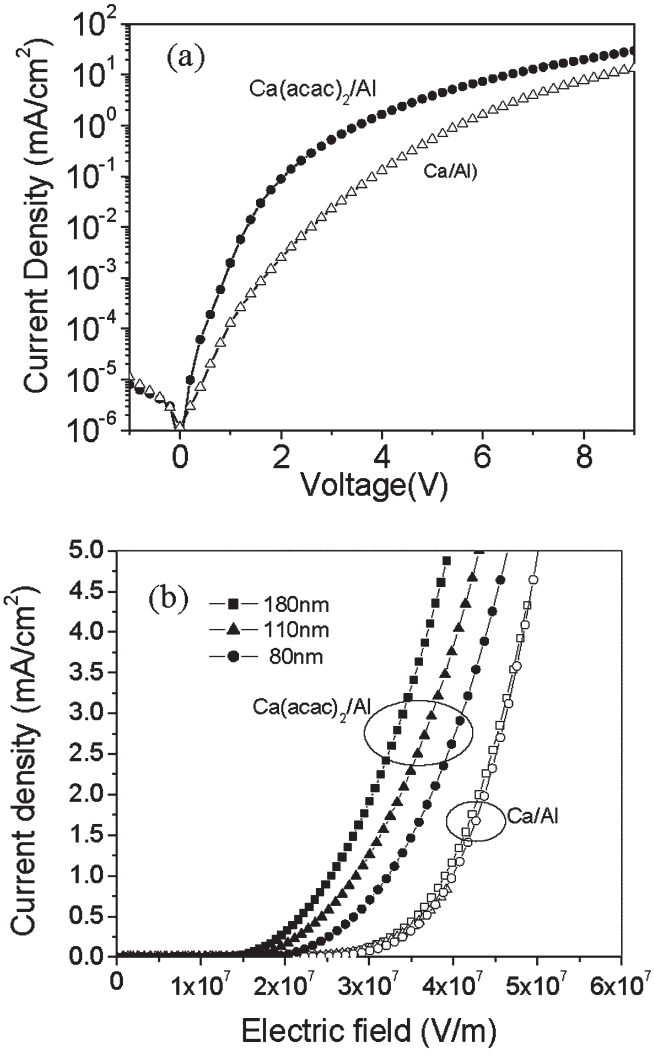

FIGURE 4 — a) The *I–V* curve comparison of electron-only devices with different cathodes: Ca(acac)$_2$/Al and Ca/Al, respectively. b) The polymer thickness dependence of I-Field (or *I–F*) curves in the electron-only devices. The square dots represent a 180-nm thickness; the triangle dots, 110-nm thickness; and round dots, 80-nm thickness.

Ca(acac)$_2$ is an insulator material with a large bandgap of about 4.3 eV (the band gap is estimated by UV-vis absorption). Therefore, the Ca(acac)$_2$ layer results in a large voltage drop across it, and one possible mechanism for the electron-injection enhancement may be due to the tunneling, similar to the case of the electron-injection layer Al_2O_3 in OLED devices. The large voltage drop on the Ca(acac)$_2$ layer helps the alignment of the LUMO of the polymer and the Fermi energy of Al, which will result in the tunneling of electrons from Al to the polymer layer. The effective energy barrier for electron injection existing in the device is thus offset by this insulating layer. This causes more electrons injected directly into the LUMO of the polymer layer through the insulating layer.

The electron-only currents were further investigated by comparing the electric-field (F) dependence of electron-only current for Ca- and Ca(acac)$_2$-based devices. From Fig. 4(b), we can find that at the same external electric field,

the current density in the $Ca(acac)_2$-based device is proportional to the thickness of the polymer layer, while the current density in Ca-based device remains almost identical for different thickness. This observation indicates that for devices using Ca/Al cathode, the electric field is totally dropped on the polymer layer, not on the electrode. On the other hand, for $Ca(acac)_2$-based device, the field is distributed on the both of the $Ca(acac)_2$ layer and the polymer layer. Usually, for a system consisting of two layers within the two electrodes (a sandwich structure), the potential (V) drop in each layer at the steady state can be calculated by the following equation:[18]

$$V_1 = \frac{(\varepsilon_2/d_2)V - \sigma}{\varepsilon_1/d_1 + \varepsilon_2/d_2}, \quad V_2 = \frac{(\varepsilon_1/d_1)V - \sigma}{\varepsilon_1/d_1 + \varepsilon_2/d_2}, \qquad (1)$$

where $V_1 + V_2 = V$, σ is the accumulated charge density, ε_i is the dielectric constant, and d_i is the thickness of the i-th layer, respectively. As can be seen, the voltage drop can be determined by the thickness, dielectric constants, as well as the accumulated charges of each layer. When the thickness of the emission polymer layer increases, the voltage drop on the insulator layer decreases, and so does the electric field. This reduces the electron injection caused by the tunneling effect. As a result, the current density changes with different polymer layer thickness in the $Ca(acac)_2$ device.

3.3 Enhanced hole injection

On the other hand, we also investigated the interfacial impact on hole injection in the various devices. In our device, the hole current is injection limited rather than space-charge limited, if we only consider the interface between the anode and polymer.[19] However, we found that the hole injection actually can also be influenced by the interface at the cathode. To clarify the situation, we removed the anode modification layer, the PEDOT:PSS. Under this condition, the energy barrier for hole injection was significantly increased, and electron injection started at a lower voltage than the hole injection. As a result, the current turn-on voltage was determined by the electron injection, while the light turn-on voltage was determined by the hole injection. Figure 5 shows the light turn-on voltage as a function of voltage and electric field at different polymer thickness. It can be seen that the light turn-on voltage in $Ca(acac)_2$ device is lower than that in Ca devices. This is strong evidence that efficient electron-injection enhances hole-injection. Earlier, we have mentioned that the electron current density in $Ca(acac)_2$ device is higher than that in the Ca device. Obviously, the accumulated electron in the polymer is proportional to electron current density [caused by the $Ca(acac)_2$ contact], particular at low operating voltage. This electron accumulation in the polymer layer has two effects in terms of hole-injection efficiency; one is to enhance the electric field to facilitate hole tunneling, the other is to reduce the energy-barrier height at the anode contact, which will also enhance the hole injection. The later effect may be

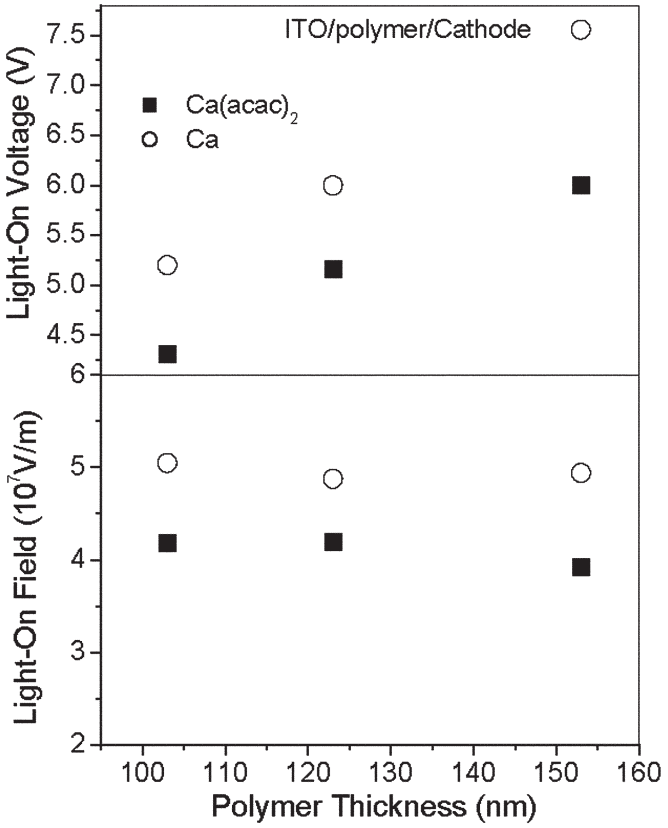

FIGURE 5 — The comparison of devices using ITO (no PEDOT) as the anode for their light-on voltage and light-on field with Ca/Al and $Ca(acac)_2$/Al cathodes under various polymer thickness.

caused by interfacial dipole.[20] Based on the Schottky effect (a mirror-image effect), the trapped electrons form an interfacial dipole layer with an electric field pointing into the polymer. This dipole can significantly lower the sharp barriers at the ITO/polymer interface.

3.4 Impedance spectroscopy measurement

To shed more light on understanding the mechanism resulting in device improvement, it is important to know the nature of the interface. AC impedance measurement has been used as a powerful tool to study the relaxation processes and internal device structures of organic and inorganic materials and devices.[25–27]

The ac impedance can be expressed as

$$Z = \frac{dV}{dI} = Z' - jZ'' = |Z|e^{i\varphi}, \qquad (2)$$

where Z' is the real part of the impedance, Z'' is the imaginary part of the impedance, φ is the phase of the complex impedance, and $|z|$ is the modulus of the impedance.

For the ac impedance, usually the imaginary part will more clearly reveal the different relaxation process presented in the devices.[29] In the logarithmic-logarithmic plot of the imaginary part, Z'', *vs.* frequency f (see Fig. 6), it is found that there is a maximum peak shown in the curves

when bias reaches 2.15 V. With the increasing bias, the curve starts to show two peaks, although not clearly separated. When bias becomes greater than 4 V, the two peaks merge into one again. The frequency of the peak position increases with the increase of bias. Moreover, with the increase of bias, the maximum values of Z'' decrease. For bias <2.15 V, the maximum peak could not be found. When frequencies are larger than 10^5 Hz, all the curves are straight lines.

From Fig. 6, in which every peak is considered as the resonance frequency of the relaxation process of the device, the equivalent circuit of the PLEDs with $Ca(acac)_2$ as interfacial layer could be considered as a serial circuit of two parallel RC components with different relaxation times (see the inset of Fig. 6), one standing for the bulk polymer layer (denoted by C_b and R_b) and the other standing for the $Ca(acac)_2$ interfacial layer (denoted by C_i and R_i). The series resistance, R_s, which is shown in the equivalent circuit is caused by the electrode contact of the devices.

In this case, we can express the complex impedance Z as

$$Z = \frac{1}{\frac{1}{R_b} + j\omega C_b} + \frac{1}{\frac{1}{R_i} + j\omega C_i} + Rs. \qquad (3)$$

After a series of mathematical transformations, the equation can be reformed to get Z' and Z'' as following:

$$Z' = \frac{R_b}{1+(C_b R_b \omega)^2} + \frac{R_i}{1+(C_i R_i \omega)^2} + Rs, \qquad (4.1)$$

$$Z'' = \frac{C_b R_b^2 \omega}{1+(C_b R_b \omega)^2} - \frac{C_i R_i^2 \omega}{1+(C_i R_i \omega)}. \qquad (4.2)$$

Moreover, from the fitted parameters (see Table 1), it could also be found that the capacitance of the bulk polymer layer increases slightly with increased bias; while that of the interfacial layer decreases dramatically. On the other hand, the resistivity of both the bulk polymer layer and the interfacial layer decrease with increased bias. The resistance values are given by the conductivity and the geometry; $R_i = \sigma_i d_i / A$. The important point is that the resistance is a strongly bias-dependent quantity, since the value of $\sigma_i = q n_i \mu_i$ changes when the carrier density n_i is increased by carrier injection, after the device is turned on; similarly, μ is also a function of bias voltage. This happens when the device is turned on. Then, it is reasonable that the resistance of both polymer layer and interfacial layer are decreased.

In the absence of doping, the values of the capacitance of each layer are determined by the geometry and the dielectric constant: $C = \varepsilon\varepsilon_0 A/d$. Ideally, it is independent of the applied bias since the dielectric constant is a bias-independent material parameter. However, owing to the presence of mobile charge carriers, the capacitance of each layer becomes a strong function of bias. The increased capacitance of the polymer bulk layer may be due to the enhanced electron injection caused by the $Ca(acac)_2$ contact. On the other hand, the decreased capacitance of the interfacial layer may be due to recombination of the electrons and holes near the interfacial region.

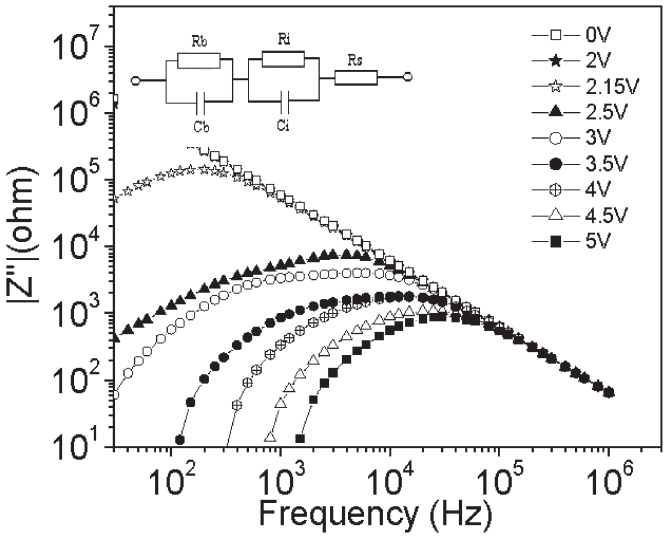

FIGURE 6 — The imagine impedance *vs.* frequency at different biases. It is noticed that there are two "peaks" on the impedance curves when the voltage is higher than 2.15 V. These two peaks suggest that the device actually consists of two layers of material with distinct electronic response.

3.5 A proposed device model

Based on the experimental results shown above, we propose a model to explain the enhancement of device quantum efficiency of our device using $Ca(acac)_2$ as the interfacial layer. When the applied voltage is small, the electrons, with assistance from the $Ca(acac)_2$ layer, are first injected into the device. The hole injection is negligible when electrons start to inject. The injected electrons subsequently enhance the hole injection by lowering the energy barrier at the anode contact. Because PFO is a hole-conducting material, and comprises 95% wt.% of the polymer, the holes are expected to be the majority carriers in the device, after the dual carrier injections happen. The excess holes migrate through the polymer bulk to the cathode and are subsequently blocked by the $Ca(acac)_2$ insulating layer. Under this circumstance, the polymer layer is charged up by electrons and holes and this significantly enhances the radiative recombination probability, if the polymer has a high fluorescence

TABLE 1 — The fitted parameters from the impedance spectra of $Z'' \sim f$ at room temperature.

T = 295K (V)	C_b (nF)	R_b (kΩ)	C_i (nF)	R_i (kΩ)
2.5	2.78	14.1	68	4.7
3	2.82	6.5	25.8	5.4
3.5	2.86	3.0	26.7	2.1
4	3.3	2.1	10.4	2.0
4.5	4.26	0.8	5.87	1.6

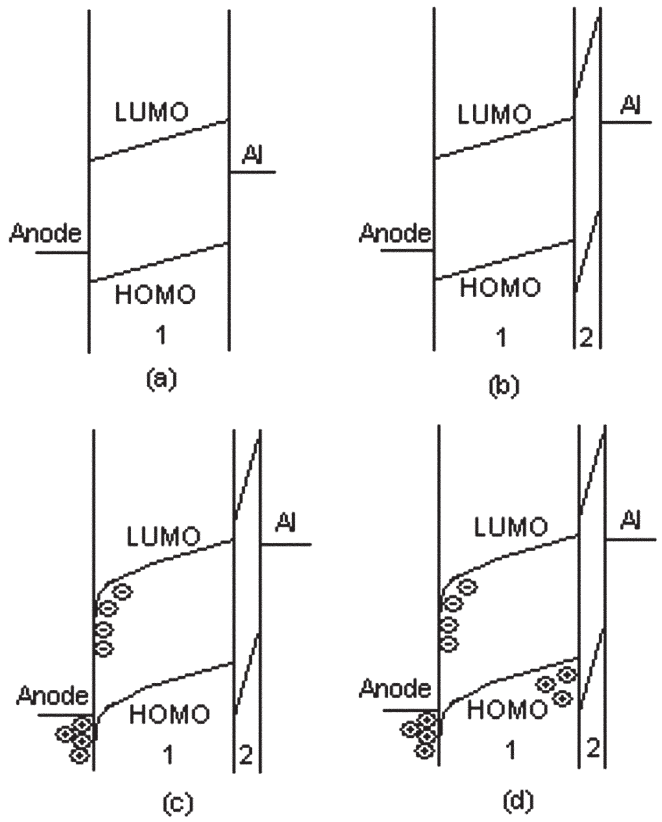

FIGURE 7 — The schematic of the device working model, layers 1 and 2 are the polymer layer and interfacial layer, respectively; (a) the device without an interfacial layer, (b) the device with a $Ca(acac)_2$ interfacial layer at the cathode contact. The majority of voltage drops on the interfacial layer, subsequently assists for the alignment of the Al electrode to the LUMO of the polymer. (c) The accumulated electrons enhance the hole injection by the interfacial dipole as well as efficient tunneling. The electrons are trapped at the green dopant polymer BT. (d) $Ca(acac)_2$ interfacial layer helps to confine the holes in the polymer layer, thus enhancing the radiative recombination process.

efficiency. This can dramatically increase the device recombination yield and therefore significantly increase the device efficiency. A simple schematic for the model is shown in Fig. 7 to illustrate this mechanism.

4 Conclusion

In summary, we have demonstrated a very-high-efficiency green polymer light-emitting diode by using a nano-scale interfacial layer to modify the cathode interface. The $Ca(acac)_2$ layer is solution processible. When overcoated with a layer of Al, they form an ideal cathode for the green polyfluorene PLEDs. This layer plays a multi-functional role. First, it provides a work function similar that of a Ca electrode. Moreover, it behaves as a thin tunneling barrier, which enhances the electron injection. In the interim, the hole injection is enhanced by the electron accumulation in the polymer layer, especially those at the region near the anode contact. This charge effect is believed to function by lowering the effective barrier height for hole injection. In addition, the $Ca(acac)_2$ layer also works as a hole block. As a result of the combination effects, the device recombination yield increases dramatically, which leads to significantly increased efficiency.

Acknowledgment

We would like to thank Prof. Junji Kido from Yamagata University, Japan, for the technical discussions and providing the green polyfluorene polymer for this work. The financial support is from the Air Force Office of Scientific Research (AFOSR, program manager, Dr. Charles Lee).

References

1 R H Friend, R W Gymer, A B Holmes, J H Burroughes, R N Marks, C Taliani, D D C Bradley, D A dos Santos, J L Breds, M Logdlund, and W R Salaneck, *Nature (London)* **397**, 121 (1999).
2 I D Parker, *J Appl Phys* **75**, 1657 (1994).
3 Y Yang, E Westerweele, C Zheang, P Smith, and A J Heeger, *J Appl Phys* **77**, 694 (1995).
4 Y Cao, G Yu, C Zhang, R Menon, and A J Heeger, *Synth Met* **87**, 171 (1997).
5 S Aratani, C Zhang, K Pakbaz, S Hoger, F Wudl, and A Heejer, *J Electron Mater* **22**, 745 (1994).
6 D Braun and A J Heeger, *Appl Phys Lett* **58**, 1982 (1991).
7 P W M Blom, M J M de Jong, and S Breedijk, *Appl Phys Lett* **71**, 930 (1997).
8 G G Malliaras and J D Scott, *J Appl Phys* **85**, 7426 (1999).
9 B K Crone, I H Campbell, P S Davids, D L Smith, C J Neef, and J P Ferraris, *J Appl Phys* **86**, 5767 (1999).
10 Y He, S Gong, R Hattori, and J Kanicki, *Appl Phys Lett* **74**, 2265 (1999).
11 K Urata, S Cinà, and N C Greenham, *Appl Phys Lett* **79**, 1193 (2001).
12 R B Fletcher, D G Lidzey, and D D C Bradley, *Appl Phys Lett* **77**, 1262 (2000).
13 L C Palilis, D I Wilkinson, D G Lidzey, D D C Bradley, M Inbasekaran, and W W Wu, *SPIE Proc* **4105**, 390 (2001).
14 A J Campbell, D D C Bradley, and H Antoniadis, *J Appl Phys* **89**, 3343 (2001).
15 E Kambe, A Ebisawa, S Shirai, and M Shinkai, Extended Abstracts, The 50th Spring Meting, The Japan Society of Applied Physics and Related Societies (2003), p. 1045.
16 Q Xu, J Ouyang, Y Yang, T Ito, and J Kido, *Appl Phys Lett* **83**, 4695 (2003).
17 I D Parker, *J Appl Phys* 1658 (1994).
18 Y E Kim, H Park, and J J Kin, *Appl Phys Lett* **69**, 599 (1996).
19 K Murata, S Cinà, and N C Greenham, *Appl Phys Lett* **79**, 1193 (2001).
20 D Poplavskyy, J Nelson, and D D C Bradley, *Appl Phys Lett* **83**, 707 (2003).
21 G G Malliaras, J R Salem, P J Brock, and J C Scott, *J Appl Phys* **84**, 1583 (1998).
22 J C Scott, G G Malliaras, W D Chen, J C Breach, J R Salem, and P J Brock, *Appl Phys Lett* **74**, 1510 (1999).
23 R N Marks, J J M Halls, D D C Bradley, R H Friend, and A B Holmes, "The photovoltaic response in poly(p-phenylene vinylene) thin film devices," *J Phys: Condens Matter* **6**, 1379–1394 (1994).
24 X Wei, S A Jeglinski, and Z V Vardeny, "Photoresponse and electroresponse studies of polymer light-emitting diodes," *Synth Met* **85**, 1215 (1997).
25 J R Macdonald, *Impedance Spectroscopy* (Wiley, New York, 1987).
26 A K Jonscher, *Dielectric Relaxation in Solids* (Chelsea Dielectrics, London, 1983).
27 K L Ngai and R W Rendell, in: *Handbook of Conducting Polymers*, edited by T A Skotheim (Dekker, New York, 1986), Chap. 28.
28 N Tessler, N T Harrison, D S Thomas, and R H Friend, *Appl Phys Lett* **73**, 732 (1998).
29 H C F Martens, W F Pasveer, H B Brom, J N Huiberts, P W M Blom, *Phys Rev B* **63**, 125328–125336 (2001).

Qianfei Xu is working as a postdoctoral fellow at the Johns Hopkins University. She holds an M.S. degree in materials science from Zhejinag University, China. She completed her Ph.D. degree in materials science and engineering under Dr. Yang Yang at the University of California, Los Angeles, where she did research on interface engineering for establishing new device architectures for organic electronic/photonic devices and further understanding of device physics. Her current research is focused on organic electrons, from materials to devices.